Effect of Varying Salt Concentration on the Behavior of Weak Polyelectrolytes in a Poor Solvent

Sahin Uyaver[†] and Christian Seidel*

Max Planck Institute of Colloids and Interfaces, Science Park Golm, D-14424 Potsdam, Germany

Received April 22, 2008; Revised Manuscript Received December 8, 2008

ABSTRACT: Using grand canonical Monte Carlo simulations of a polyelectrolyte chain where the charges are in contact with a reservoir of constant chemical potential given by the solution pH, we study the behavior of weak polyelectrolytes in a poor solvent. We address the influence of variable screening of the electrostatic interaction on the chain structure for rather poor solvents as well as in the close-to-Θ-point regime. For the latter case, we demonstrate that a fine tuning of the chain structure is attainable by varying screening. With growing screening length, that is, by reducing the salt concentration, the degree of charging is reduced and the pearl distribution can be shifted toward a smaller number of pearls. In addition, we find that pearl necklaces can also occur at high charging provided the screening is very strong. In the rather-poor-solvent regime, the position of the discrete transition from a highly charged, stretched chain to a weakly charged globule can be shifted by the variation of screening. By reducing the screening of electrostatic repulsion, we observe in both regimes a nonmonotonic stretching of the polyelectrolyte. After reaching a maximum of stretching, the chains relax back to an asymptotic value at vanishing screening, which depends on pH. For rather poor solvents, at large screening lengths, the chains collapse into an almost uncharged globule provided that high ionization is not pinned by a large chemical potential of the charges.

1. Introduction

Polyelectrolytes (PELs) are macromolecules that contain subgroups that have the ability to dissociate charges in polar solvents such as water. In recent years, PELs have received much attention because of their importance in materials science, soft matter research, and molecular biology. The combination of polymer properties and electrostatic interactions can result in competing interactions and gives rise to quite different length scales. This complexity also makes PELs interesting from a fundamental point of view. Despite considerable effort, understanding PELs still constitutes a challenging area for both fundamental and applied studies.[1−3] With respect to different dissociation behavior, one can distinguish between strong and weak PELs, a classification that is widely used in the chemistry community[1] or between quenched and annealed PELs, the common classification of the same polymers used in the physics community.[2]

Strong polyelectrolytes, for example, poly(sodium styrene sulfonate), completely dissociate in the total pH range accessible by experiment. The total charge as well as its particular distribution along the chain is solely imposed by polymer synthesis. Therefore, in the language of statistical mechanics of disordered systems, the charge distribution is a quenched variable. However, weak PELs, for example, poly(acrylic acid), dissociate in only a limited pH range. The total charge of the chain is not fixed but can be tuned by changing the pH. The number of charges $N_c = fN$ (where N is the number of monomers and f is the degree of ionization) as well as their positions are fluctuating thermodynamic variables. The imposed quantity is the chemical potential of the charges. At high dilution and constant salt concentration, it equals the pH of the solution up to a trivial additive constant. In this case, the distribution of charges is an annealed variable. Because of dissociation and recombination of ion pairs, the charges can effectively move along the chain. This extra degree of freedom gives rise to new and nontrivial features. The specific behavior of weak PELs has attracted considerable interest in experimental,[4−10] theoretical,[11−15] and simulation studies.[16−23]

Many polymers are based on a hydrophobic hydrocarbon backbone, and the solubility of PELs in water is often only given by charged side groups. The competition between the attractive monomer−monomer interaction due to a poor solubility of the backbone and the repulsive Coulomb interaction between the polymer charges gives rise to a rather complex phase behavior of PELs in poor solvents. To minimize the interfacial area with the solvent, an uncharged hydrophobic polymer immersed in water forms a globule.[24,25] After adding charges to the polymer, the globule loses its spherical shape[26] and can form so-called pearl necklaces, locally collapsed structures (pearls) connected by elongated strings.[27−31]

For annealed PELs in a poor solvent, the charge degree of freedom can have a strong effect on the behavior of the polymer. A first-order phase transition between weakly charged globules and a strongly charged stretched chain predicted by theory[11] was confirmed by simulations.[20] For sufficiently poor solvent quality, the behavior of the polymer is dominated by this transition, which is reflected in pronounced anomalies of the titration curves of, for example, poly(methacrylic acid)[4,5] and poly(maleic acid).[6] However, if the system is close to the Θ point, then the discontinuous phase transition is suppressed and intermediate structures such as pearl necklaces can be stable.[3,11] Analyzing the conformational changes of poly(vinylamine) caused by a tuning of polyelectrolyte charge through the variation of the solution pH, recently direct evidence was found of the existence of pearl necklaces in annealed PELs.[31] Similarly, a cascade of pearl necklace transitions was obtained by simulations in the close-to-Θ-point regime.[21] At a certain degree of charging, the pearl necklaces obey the predictions made by Dobrynin, Rubinstein, and Obukhov (DRO)[29] for the case of quenched PELs. However, the region where the particular structures are stable is rather restricted.

In this Article, we study the influence of a varying screening of the electrostatic interaction between polymer charges on

* To whom correspondence should be addressed. E-mail: seidel@mpikg.mpg.de.
[†] Present address: T.C. Maltepe Üniversitesi, Istanbul, Turkey.

10.1021/ma801817j CCC: $40.75
Published on Web 01/26/2009

dissociation behavior and the structure of annealed PELs in both the deep-poor-solvent regime and the close-to-Θ-point regime. Although the fundamental behavior is determined by the solvent quality measured by the dimensionless distance from the Θ point, $\tau = 1 - T/\Theta$, and the solution pH, some fine tuning can be enforced by changing the screening length $\lambda_D = (8\pi c_s \lambda_B)^{-1/2}$, where c_s is the salt concentration (1:1 electrolyte) and $\lambda_B = e^2/4\pi\varepsilon_0\varepsilon k_B T$ is the Bjerrum length that determines the strength of the Coulomb interaction. For annealed PELs in good solvents, it is known that λ_D sets the length scale over which the local charge density is enhanced close to chain ends.[12,18,19] In the close-to-Θ-point regime, we find that the pearl necklace population can be manipulated by varying screening. In addition to the DRO pearl necklace regime where the necessary weakness of Coulomb repulsion is reached by a sufficient decrease in the degree of charging, we obtain a second regime with $f = 1$ but at rather strong screening of $\lambda_D < b$, with b being the distance between ionizable groups. Because of the decreasing degree of charging, the chain size can shrink with growing λ_D, which is contrary to the usual polyelectrolyte effect. Thus, as a whole, we find a nonmonotonic dependence of chain size on ionic strength. Upon increasing λ_D in the rather-poor-solvent regime, we find discrete transitions to weakly charged globules provided that the ionization is not pinned at $f \lesssim 1$ because of a large chemical potential of the charges. Independent of the solvent quality, for completely charged chains, we observe an almost perfect agreement with the behavior of a persistent blob chain predicted by Khokhlov and Khachaturian.[32]

Note that a similar nonmonotonic behavior of surface pressure or brush height on ionic strength was found for phospholipid membranes[33] and polyacid brushes,[34] respectively. However, although it is also an effect due to the annealing of charges, the underlying physics is different. Whereas in inhomogeneous systems such as membranes or brushes the distribution of protons and salt ions close to the interface plays the dominating role, in dilute polyelectrolytes, it is due to intramoleclular electrostatic interaction.

The outline of the Article is as follows: In section 2, we give a brief review of the theory of PELs in poor solvent, the effects of annealed charge distribution and screening. Simulation model and method are introduced in section 3. In the following section, the simulation results are discussed, and a brief summary as well as our conclusions can be found in section 5.

2. Theory

2.1. Strong Polyelectrolytes in a Poor Solvent. To minimize its interfacial energy, uncharged polymers in a poor solvent collapse into a dense globule.[24,25] The monomer density inside the globule becomes $\rho_{glob} \simeq \tau/b^3$, with τ being the normalized distance from the Θ point, which is a measure of the solvent quality, and the polymer chain has N monomers of size b. On length scales that are smaller than the thermal correlation length, $\xi_T \sim b/\tau$, attractive interactions are not relevant, but Gaussian fluctuations dominate the behavior of the polymer. The globule can be understood to consist of densely packed thermal blobs of size ξ_T, and its total size becomes $R_{glob} \sim (N/\rho_{glob})^{1/3} \approx bN^{1/3}/\tau^{1/3}$. For most purposes, the globule can be viewed as a liquid droplet. The connectivity of the chain does not play any important role. The free energy of the globule is governed by the interfacial contribution resulting in a surface tension $\gamma \sim k_B T/\xi_T^2 \sim \tau^2$. For finite chain length, there exists a region close to the Θ point given by $\tau < \tau_0^* \sim 1/N^{1/2}$ where Gaussian fluctuations dominate the whole chain.

With the growing degree of charging f (in this subsection, considered to be fixed), the globule will spontaneously deform at $f = f_c \sim (\tau/uN)^{1/2}$, where Coulomb repulsion, $F_{Coul} \sim k_B T f^2 N^2 \lambda_B/R_{glob}$, becomes comparable to surface energy, $F_{sur} \sim \gamma R_{glob}^2$. Using the concept of electrostatic blobs, a simple description of the deformation of a charged globule was given by Khokhlov.[26] The blob size, ξ_e, determined by the balance of the electrostatic energy of the blob and its surface energy, reads $\xi_e \sim b/(uf^2)^{1/3}$, where $u = \lambda_B/b$ is a dimensionless interaction parameter. On length scales larger than ξ_e, electrostatics dominates the structure. The blobs repel each other and form an elongated chain of width ξ_e and length[26]

$$R_{cyl} \sim bN(uf^2)^{2/3}/\tau \tag{1}$$

Later, Dobrynin, Rubinstein, and Obukhov[29] showed that cylindrical globules are unstable against the Rayleigh instability.[27] The chain lowers its free energy by forming a so-called pearl necklace structure that consists of $n_p \sim Nuf^2/\tau$ collapsed globules of size ξ_e connected by narrow strings of thickness ξ_T that are stretched by the electrostatic repulsion between pearls. The total length of the pearl necklace becomes

$$R_{nec} \sim bN(uf^2/\tau)^{1/2} \tag{2}$$

Note that deep in the poor solvent regime at $\tau > uf^2N$ the chain collapses into a single globule. However, close to the Θ point at $\tau < (uf^2)^{1/3}$, the chain behaves like a charged polymer in Θ solvent; that is, it exhibits the configuration of a homogeneously stretched blob chain with[35]

$$R_\Theta \sim bN(uf^2)^{1/3} \tag{3}$$

2.2. Weak or Annealed Polyelectrolytes. For annealed polyelectrolytes, the fraction, f, of charged monomers is not fixed but determined by the minimum of the grand canonical free energy, that is, the free energy at constant charge chemical potential, μ. At infinite dilution, in a mean field approach, the corresponding thermodynamic potential reads[11]

$$\frac{F(f)}{k_B T} = N[f \ln f + (1-f)\ln(1-f) + f\mu] + \frac{F_e(f)}{k_B T} \tag{4}$$

The first two contributions are ideal gas mixing entropy for charged and noncharged monomers along the chain, the third term is the charge chemical potential term, and the last term is the total electrostatic free energy of the chain, which depends on its structure.[11,12] The bulk charge chemical potential is imposed by the solution pH via[11]

$$\mu = \mp \ln 10\,(\mathrm{pH} - \mathrm{p}K_0) \tag{5}$$

where $\mp$ stands for acid/base and pK_0 is the intrinsic dissociation constant of an isolated monomer. Using $\mathrm{pH} - pK_0$ as an input parameter, in most of the simulation studies on annealed polyelectrolytes,[17,18,22] eq 5 is applied to calculate the change in energy due to protonation/deprotonation. Netz pointed out that at finite screening, the self energy of a released proton gives an additional contribution to the chemical potential, and eq 5 becomes[14]

$$\mu = \mp \ln 10\,(\mathrm{pH} - \mathrm{p}K_0) - \lambda_B/\lambda_D \tag{6}$$

Note that at infinite polyelectrolyte dilution, the effect of counterions can be neglected and the screening length is solely determined by the salt concentration. By minimizing eq 4 with respect to the charge fraction f, one obtains the titration law as

$$\mu(f) = \ln\frac{1-f}{f} - \mu_e(f) \tag{7}$$

where $\mu_e(f) = (k_B T N)^{-1}\partial F_e(f)/\partial f$ is the electrostatic contribution to the chemical potential. Note that eqs 5−7 can be written in the form[22]

$$\mathrm{pH} - \mathrm{p}K_0 - \Delta\mathrm{p}K(f) = \log_{10}\frac{f}{1-f} \tag{8}$$

where $\Delta pK(f)$ actually contains both the difference between the dissociation constant of an isolated and a bound monomer and the self-energy contribution.

Obviously, the charge chemical potential has two different contributions: an entropic contribution and an electrostatic contribution. For good and Θ solvents, the electrostatic contribution is an increasing monotonic function of f. Thus, for a given pH, the fraction of charges, f, is well defined, and the properties of the chains are very similar to those of quenched polyelectrolytes except for a nonhomogeneous charge distribution close to chain ends.[12,19] However, in a sufficiently poor solvent with

$$\tau > \tau_a^* \sim (u^3 N)^{-1/5} \tag{9}$$

the cylindrical blob model discussed above gives a nonmonotonic variation of μ with f, which indicates a transition between a weakly charged globular structure and a highly charged stretched chain.[11] This transition occurring at a certain chemical potential, μ^*, is of first order.[11,20,23] Considering the pearl necklace conformation, Castelnovo et al.[12] obtained exactly the same stability criterion as that given in eq 9. The coincidence appears because the leading terms of the free energy are identical for cylindrical globules and pearl necklaces, respectively, and different prefactors are ignored in a scaling type approach.

Therefore, the general picture for annealed polyelectrolytes in a poor solvent is: (i) For sufficiently poor solvent quality $\tau > \tau_a^*$, at a certain chemical potential, μ^*, they undergo a first-order phase transition between weakly charged globules and strongly charged, stretched chains. (ii) In the intermediate range, $\tau_0^* < \tau < \tau_a^*$, which is usually called the close-to-Θ-point regime, the transition between globule and stretched chain becomes almost continuous in f and R. Although, with the growing degree of charging, there occurs a sequence of discrete pearl necklace transitions embedded in the continuous crossover; because of strong fluctuations, the pearl necklace transition as a whole appears to be continuous. Recently, this prediction could be confirmed by extensive Monte Carlo simulations[21] (iii) In the direct vicinity of the Θ point at $\tau < \tau_0^*$, henceforth called the Θ regime, the chain is expected to exhibit a continuous crossover from an uncharged Gaussian one at $\mu = 0$ to a strongly charged, stretched blob chain at large chemical potential.

2.3. Effect of Additional Salt. When salt is added to a dilute solution of PELs, the electrostatic interaction between charged monomers becomes short-ranged and can be described by the Debye−Hückel (DH) potential

$$U_{DH}(r) = k_B T \frac{\lambda_B}{r} \exp(-r/\lambda_D) \tag{10}$$

with λ_D being the Debye screening length introduced above. A complete scaling picture of the dependence of PEL solutions on salt concentration was given by Schiessel.[36] Depending on the ionic strength, λ_D can typically vary from <1 to >100 nm. Whereas on separations smaller than λ_D screening can be neglected, distant parts of the chain do not interact, and in the limit of large N, the polymer is expected to behave as a neutral one with electrostatically modified short-ranged interactions. Thus, varying the salt concentration is a convenient tool for tuning the conformation of PELs. In a very simple way, the effect of short-ranged electrostatic interaction in PEL solutions with additional salt can be described by two parameters: the electrostatic persistence length, l_e, and the electrostatic excluded volume, v_e. Actually, l_e may be much larger than λ_D, a fact that is well known for intrinsically stiff polyelectrolytes ($l_0 \gg b$, with l_0 being the persistence length of the underlying neutral chain) such as DNA. Note that from a microscopic point of view the model we are applying is rather crude. The water molecules are modeled by a high-dielectric continuum ($\varepsilon = 80$), and within the DH approach, low-molecular ions are smeared out to a continuous background. Although electrostatic interaction is different for collapsed chains within low-dielectric globules and extended configurations in a high-dielectric solvent, respectively, for simplicity, we assume the same interaction strengths as well as screening lengths for all possible structures. Nevertheless, such a crude model captures the basic features of polyelectrolytes in solution.

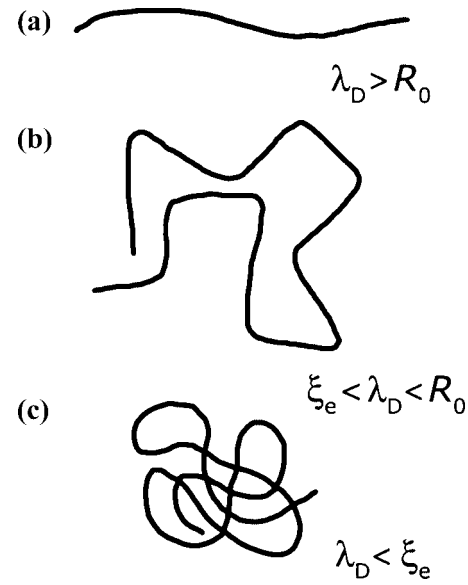

Figure 1. Transition from a flexible polyelectrolyte chain to a highly stretched one with growing screening length, λ_D, where R_0 is Gaussian coil size and ξ_e is the electrostatic correlation length: (a) $\lambda_D > R_0$, (b) $\xi_e < \lambda_D < R_0$, (c) $\lambda_D < \xi_e$.

Depending on salt concentration, PELs exhibit regimes of quite different behavior. To illustrate the basic features, we consider intrinsically flexible quenched PELs ($l_0 \ll b$) in the Θ regime. At large Debye lengths, $\lambda_D \gg R_0 \sim bN^{1/2}$, screening is unimportant and PELs form elongated blob chains (Figure 1a) of size R_Θ given by eq 3. However, at $l_e \approx R_\Theta$ or $\lambda_D \approx R_0$, screening comes into play. The blob chain of contour length R_Θ is no longer completely elongated but can be seen as a flexible chain built by cylindrical monomers of length l_e and diameter λ_D. (See Figure 1b and regime 4_s in ref 36). Following Odijk and Houwaart,[37] the segment−segment interaction gives a second virial coefficient

$$v_e \sim l_e^2 \lambda_D \tag{11}$$

which is called electrostatic excluded volume. On a Flory mean-field level, the size of the chain becomes

$$R \sim (v_e l_e^2)^{1/5} \tilde{N}^{3/5} \sim (l_e \lambda_D)^{1/5} \tilde{L}^{3/5} \tag{12}$$

where $\tilde{N} = \tilde{L}/l_e$ is the number of rigid segments with $\tilde{L} = R_\Theta$ being the contour length of the blob chain. For intrinsically stiff PELs, l_e is given by the well-established Odijk−Skolnick−Fixman (OSF) theory as[2,38,39]

$$l_e \sim u f^2 \lambda_D^2 / b \tag{13}$$

For flexible PELs, however, there is a long debate about the correct relation between persistence length, l_e, and screening length, λ_D.[2,32,40,41] Without going into the details, we use the following general relation

$$l_e \sim b(\lambda_D/b)^{\alpha} \tag{14}$$

where the free exponent α will be fitted by the simulation data. Using eqs 3 and 14, eq 12 yields

$$R_{s1} \sim bN^{3/5}\left(\frac{\lambda_D}{b}\right)^{\frac{1+\alpha}{5}}, \quad \xi_e < \lambda_D < R_0 \tag{15}$$

Setting $\alpha = 2$, eq 15 gives the OSF result predicted by Khokhlov and Khachaturian.[32]

Upon a further increase in salt concentration, the concept of electrostatic blobs becomes irrelevant at $\lambda_D < \xi_e$, and PELs behave as flexible chains. (See Figure 1c.) In this regime, the size of the chain can be calculated by means of usual excluded volume theory of flexible chains.[32] The screened Coulomb interaction yields an electrostatic excluded volume

$$v_e \sim f^2 \lambda_B \lambda_D^2 \tag{16}$$

and the chain size becomes[32]

$$R_{s2} \sim bN^{3/5}(\lambda_D/b)^{2/5}, \quad b < \lambda_D < \xi_e \tag{17}$$

Therefore, with respect to λ_D, there appears to be slightly different scaling at $\lambda_D > \xi_e$ or $\lambda_D < \xi_e$ as soon as $\alpha > 1$.

In the limit of strong screening, under poor solvent conditions, the electrostatic excluded volume directly competes with short-ranged attraction, and the behavior of PELs is governed by an effective excluded volume[42]

$$v_{eff} \sim b^3\left(uf^2\lambda_D^2/b^2 - \tau\right) \tag{18}$$

For small τ, v_{eff} is positive, but it becomes negative at $\lambda_D^2 < b^2\tau/(uf^2)$. Therefore, driven by additional salt, the chain smoothly changes from a swollen to a collapsed state passing through an effective Θ point.

At intermediate screening, in a poor solvent, the behavior is very similar to that discussed above in the close-to-Θ-point regime. Instead of R_Θ, the contour length of the blob chain is then given by the poor solvent relation eq 1. However, the resulting expression differs from eq 12 only by some prefactors.[36] Note that one obtains similar scaling behavior even for more sophisticated models that include poor solvent scaling within electrostatic blobs,[42] or take into account pearl necklace structures.

Theoretical predictions on the specific influence of additional salt in annealed polyelectrolytes are rather rare. Starting from a partially ionized state, the degree of charging should grow with increasing salt concentration because the electrostatic penalty of ionization is reduced. The change is expected to be continuous in the close-to-Θ-point regime but might be discontinuous at $\tau > \tau_a^*$. For sufficiently high salt concentration, any anomaly of annealed polyelectrolytes in poor solvents should disappear because the chemical potential is governed by the entropic contribution that is monotonically growing with f.[42] In this case, there remain only end effects over lengths on the order of λ_D, which is well known from previous studies.[12,19]

3. Simulation Model and Method

The polymer is represented by a freely jointed bead-spring chain. Along the chain, the monomers are connected to their neighbors by a harmonic bond potential

$$U_{bond}(r) = \frac{3}{2}k_B T\frac{r^2}{b_0^2} \tag{19}$$

with b_0 being the (bare) average bond length. The nonelectrostatic interactions between the monomers, which effectively also include the interaction with solvent molecules, are modeled by a modified Lennard-Jones potential, where the interaction at distances $r \leq r_c = 2^{1/6}\sigma$ is given by

$$U_{LJ}(r) = 4\varepsilon\left\{\left[\left(\frac{\sigma}{r}\right)^{12} - \left(\frac{\sigma}{r}\right)^{6} + \frac{1}{4}\right] + \beta\left[\cos\frac{2\pi r}{r_c} - 1\right]\right\} \tag{20}$$

and is zero elsewhere.[43] This potential contains a very narrow attractive part such that the range of interaction remains short. The strength of the attractive interaction is set by the parameter β. We use b_0 as the unit of length, ε as the unit of energy, and the monomer mass, m, as the unit of mass. All quantities are expressed in this unit system. To ensure that the bond length distribution remains almost Gaussian, we set $\sigma = {}^1/_2$. Simulations were performed at temperature $k_BT = 1.2$. In addition to short-range interactions, all charged monomers interact with each other via a screened Coulomb (Debye−Hückel) potential given in eq 10.

Because we are studying polyelectrolytes at infinite dilution, the screening length, λ_D, is determined only by the concentration of added salt and not by polymer charges and counterions. That is why λ_D can be considered to be constant at varying μ. The exponentially decaying interaction enables the introduction of a cutoff that we choose as $\lambda_c = 5\lambda_D$. If not otherwise stated in the simulations reported here, then the chain length is $N = 256$ and the screening length is tuned between 0.05 b_0 and 1024 b_0.

Varying the parameter β is equivalent to changing the solvent quality: the larger the value of β, the poorer the solvent quality. At $\beta = \beta_\Theta$, the short-range attractive interactions compensate for the repulsive ones, and the uncharged chain becomes Gaussian with a coil extension $R_0 \sim N^{1/2}b$. For the parameter set used, we found $\beta_\Theta = 2.615 \pm 0.015$.[20] Within our model, the normalized distance from the Θ point is given by

$$\tau = \frac{\beta}{\beta_\Theta} - 1 \tag{21}$$

Equilibrium properties are studied by standard Metropolis Monte Carlo (MC) simulation. To equilibrate both long and short length scales, we combine three different configurational MC moves: (i) pivot, (ii) reptation, and (iii) local displacement. Annealed PELs are simulated in a grand canonical ensemble in which the chain is in contact with a reservoir of charges of fixed chemical potential μ.[19] Exactly speaking, the ensemble is a semigrand canonical one in which the total number of particles (monomers) is fixed but the number of particles that carry a charge is fluctuating. In addition to the configurational MC moves introduced above, the algorithm is completed by a charge move by which the charge state of a randomly chosen monomer is switched. The energy change of a complete MC move reads

$$\Delta E = \Delta E_c \pm \mu \tag{22}$$

where ΔE_c is the change in configurational energy

$$\Delta E_c = \Delta U_{bond} + \Delta U_{LJ} + \Delta U_{DH} \tag{23}$$

The plus sign in eq 22 is used when the monomer is to be neutralized (protonated), and the minus sign is used when it is to be charged (deprotonated).

To ensure that the simulation generates equilibrium data, we start with three quite different configurations: (i) random coil, (ii) dumbbell, and (iii) globule and require that after appropriate relaxation they yield identical averaged quantities. Depending on the type of starting configuration, different mixing of the elementary MC moves is necessary. Details of the simulation routes as well as of statistical errors can be found elsewhere.[21] Finally, the relative error of the m.s. end-to-end distance $R = \langle R^2\rangle^{1/2} = \langle (r_N - r_1)^2\rangle^{1/2}$ was shown to be $<1\%$ in the collapsed state and $<8\%$ in the extended state. The number of charges

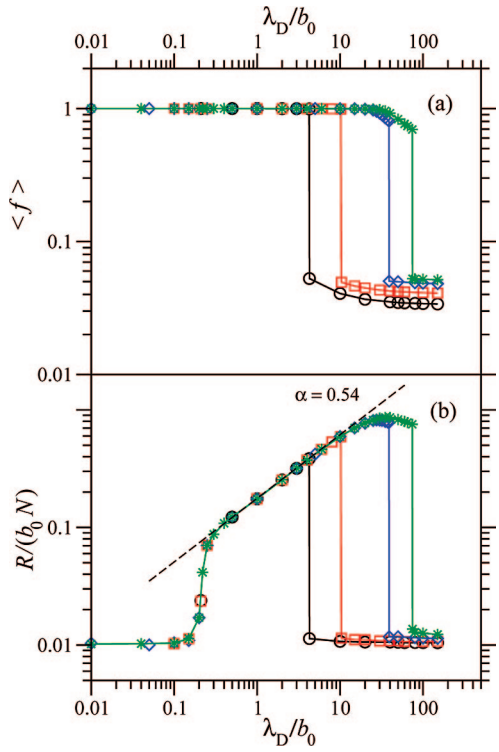

Figure 2. Simulation results at $\tau = 0.19$ ($N = 256$, $\lambda_B = b_0$) and varying chemical potential: $\mu = 5.0$ (○), 6.0 (□), 7.0 (◇), and 7.41 (∗). (a) Average degree of charging versus screening length and (b) m.s. end-to-end distance versus screening length. The dashed line gives the best fit by a power law.

are reproducible within <1% independent of the conformation of the polyelectrolyte.

4. Simulation Results

Recently, the theoretically predicted behavior of annealed PELs in a poor solvent could be confirmed by numerical simulations.[20,21,23] In the rather-poor-solvent regime, $\tau > \tau_a^*$, with τ_a^* being given by eq 9, the chains undergo a first-order phase transition between weakly charged globules and highly charged stretched conformations. Intermediate structures, in particular pearl necklaces, exist in the close-to-Θ-point regime, $\tau < \tau_a^*$. For chains of length $N = 256$, at $\lambda_B = 1.0$, the characteristic solvent quality becomes $\tau_a^* \approx 0.3$. Note that eq 9 is based on a scaling theory approach, that is, any numbers are omitted. In a previous paper,[20] it was shown that at $\tau = 0.19$ ($\beta = 3.11$), the PELs exhibit strong poor-solvent behavior with a pronounced first-order phase transition. However, at $\tau = 0.07$ ($\beta = 2.80$), a sequence of pearl necklace transitions has been observed with growing chemical potential.[21] In both studies, the screening length was fixed at $\lambda_D = 10b_0$. In the following, the influence of varying screening is analyzed in detail in both poor solvent regimes. Note that the influence of varying screening can be experimentally studied rather easily by tuning the salt concentration. At very high salt concentrations, that is, at $\lambda_D \ll b_0$, the electrostatic interaction is completely suppressed and charged chains exhibit the behavior that is known for neutral chains.

4.1. Rather-Poor-Solvent Regime. Figure 2 shows both degree of charging and mean-square end-to-end distance as a function of screening length, λ_D. Typical snapshots that illustrate chain structure in the different regions can be found in Figure 3. With growing screening length, we observe five different regimes: (i) For very small screening lengths, $\lambda_D/b_0 < 0.1$, the polyelectrolyte is completely charged at any (positive) chemical potential. Nevertheless, the chain remains a globular structure because electrostatic interactions are completely suppressed. (ii) For $0.1 < \lambda_D/b_0 < 0.3$, the chain remains completely ionized. Because of finite electrostatic excluded volume, the chain structure is continuously changed from a globule to a swollen coil. (iii) For $0.3 < \lambda_D/b_0 < 10$, except for some fluctuations, the chain remains almost fully ionized; that is, it practically exhibits the behavior of a quenched polyelectrolyte. With growing λ_D, the coil becomes increasingly swollen, obeying a scaling law $R \approx \lambda_D^{0.54}$. Using eq 15, the exponent α that governs the electrostatic persistence length (see eq 14) is found to be $\alpha = 1.7$, a value that is a bit smaller than the OSF prediction $\alpha = 2$. Evaluating the structure factor, below we will see that the underlying scaling behavior of a semiflexible chain, $R \sim N^{3/5}$, is fulfilled in a large range of regime iii; that is, the application of eq 15 is justified in the particular regime. (iv) For $10 < \lambda_D/b_0 < \lambda_D^*/b_0$, partial neutralization of the chain becomes energetically favorable. Concerning chain size, there is a competition between an enhancement of the polyelectrolyte effect due to growing screening length and a suppression due to the reduced degree of dissociation. This is why R exhibits a nonmonotonic behavior with growing λ_D. (v) At $\lambda_D = \lambda_D^*(\mu)$, the chain undergoes a discrete transition to an almost uncharged globule. In previous studies,[20,23] it was shown that this type of transition is of first order. Note that for our choice of τ regime iv is missing if $\lambda_D^*(\mu) < 10b_0$. In this case, there appears to be a discrete transition from a fully charged coil to an almost neutral globule. The transition points $\lambda_D^*(\mu)$ are given in Table 1. Therefore, at constant solvent quality, τ, interaction strength, u, and solution pH, there is another way to switch the configuration of annealed PELs between a highly charged stretched state and a weakly charged globule, namely, by tuning screening length, λ_D; that is, by changing the ion strength of the solution. In other words, the solution pH at which an annealed PEL undergoes a discontinuous transition to a weakly charged globule can be adjusted to a certain value by choosing the right salt concentration. Note that at a given solvent quality, τ, and finite chain length, N, there exists a maximum chemical potential above which annealed PELs do not undergo a transition to a weakly charged globule at any λ_D. At $\tau = 0.19$ and $N = 256$, the limiting value is $\mu = 7.41$.

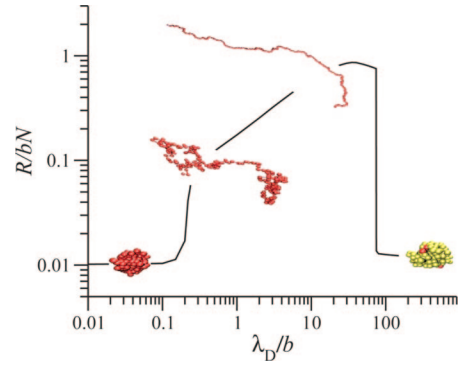

Figure 3. Typical simulation snapshots ($\tau = 0.19$, $\mu = 7.41$) demonstrating a varying conformation with increasing screening length $\lambda_D/b_0 = 0.01$, 0.3, 10, 100. Charged monomers are colored red and uncharged monomers are colored yellow.

Table 1. Transition Point λ_D^* in the Rather-Poor-Solvent Regime ($N = 256$, $\tau = 0.19$)

μ	λ_D^*/b_0
5.0	4.25 ± 0.03
6.0	10.2 ± 0.1
7.0	38.9 ± 0.1
7.41	74.3 ± 0.4

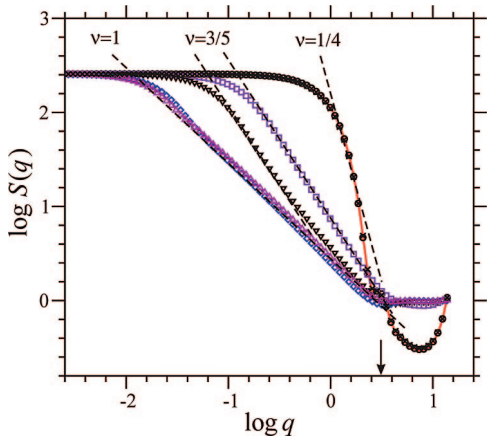

Figure 4. Spherically averaged structure factor ($\tau = 0.19$, $\mu = 7.41$) at varying screening length: $\lambda_D/b_0 = 0.01$ (−), 0.1 (○), 0.3 (□), 1.0 (▽), 10 (◇), 74.5 (△), 100 (×). Dashed lines show particular scaling behavior. The arrow indicates the position of a peak related to globule size.

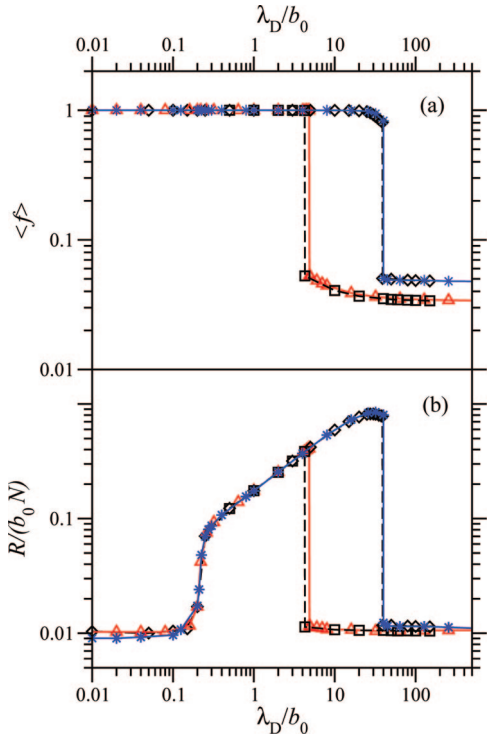

Figure 5. Simulation results at $\tau = 0.19$ ($N = 256$, $\lambda_B = b_0$). Shown are (a) average degree of charging versus screening length and (b) m.s. end-to-end distance versus screening length, both at $\mu = 5$ (□), pH−pK_0 = 2.17 (△), and $\mu = 7$ (◇), pH−pK_0 = 3.04 (∗).

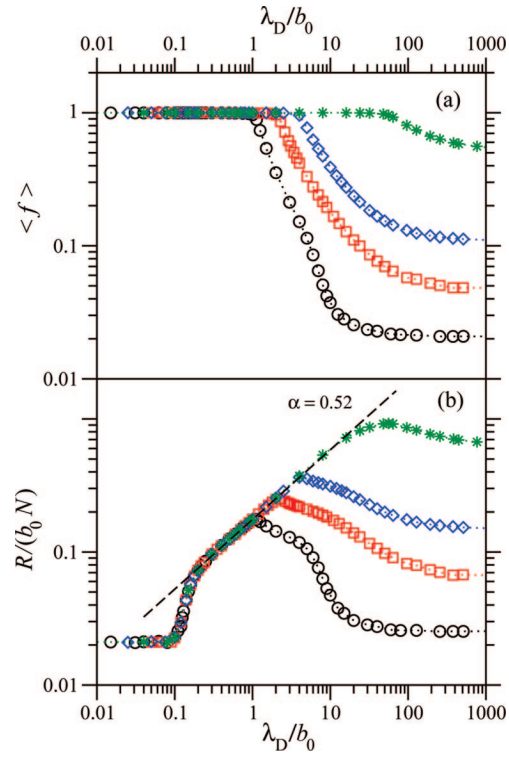

Figure 6. Simulation results at $\tau = 0.07$ ($N = 256$, $\lambda_B = b_0$) and varying chemical potential: $\mu = 2.0$ (○), 3.0 (□), 4.0 (◇), and 8.0 (∗). (a) Average degree of charging versus screening length and (b) m.s. end-to-end distance versus screening length. The dashed line gives the best fit by a power law.

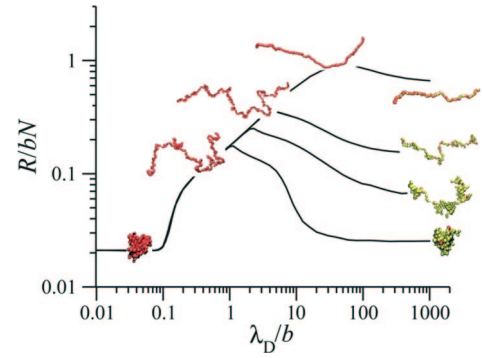

Figure 7. Typical simulation snapshots ($\tau = 0.07$) demonstrating a varying conformation with increasing screening length. The branches on the right belong to different chemical potentials $\mu = 2, 3, 4, 8$ (from bottom to top). (See Figure 6.) Note that below $\lambda_D/b_0 = 1$ the chains are more or less completely ionized. Charged monomers are colored red and uncharged monomers are colored yellow.

For $\mu = 7.41$, in Figure 4, we plot the spherically averaged structure factor for a set of characteristic screening lengths. It shows the effect of additional salt on different length scales. Below $\lambda_D/b_0 = 0.1$ (regime I discussed above), there is no effect at all and the structure factor exhibits a clear peak at $q \approx 3.2$ related to globule size $R_{glob} \approx 2.0$. At $\lambda_D/b_0 = 0.3$, the structure factor gives a Flory exponent $\nu \approx 0.6$, indicating a swollen coil caused by electrostatic excluded volume. At intermediate screening $0.3 < \lambda_D/b_0 < 10$, there appear two different scaling regimes. On large length scales, one still obtains swollen coil behavior, whereas on short length scales, the chain becomes increasingly stiff. (See $\lambda_D/b_0 = 1$ in Figure 4.) This gives some insight into regime iii that was not seen in the R versus λ_D dependence plotted in Figure 2. With growing screening length, the large q regime is extended, and at $\lambda_D/b_0 = 10$, the whole chain is more or less homogeneously stretched with a Flory exponent that becomes close to $\nu = 1$. Finally, at $\lambda_D > \lambda_D^* \approx 74.5$, the chain collapses back into a globule that is almost uncharged but otherwise identical to that obtained in the strong screening limit. Note that shrinking obtained in the mean-square end-to-end distance at $\lambda_D/b_0 > 40$ (see Figure 2) occurs not because of a weaker overall stretching but because of a wiggling on short lengths for partially charged chains. A detailed analysis of $S(q)$ at $\lambda_D = \lambda_D^* \approx 74.5 b_0$ shows that the swelling exponent becomes $\nu = 1$ on large length scales, whereas reduced stretching with $\nu \approx 0.8$ to 0.9 is obtained on short scales.

So far, the chemical potential of the charges was considered to be identical to the solution pH, except for a constant term λ_B/λ_D. (See eq 6.) Obviously this is not true as soon as λ_D is not fixed. Therefore, considering the chemical potential to be

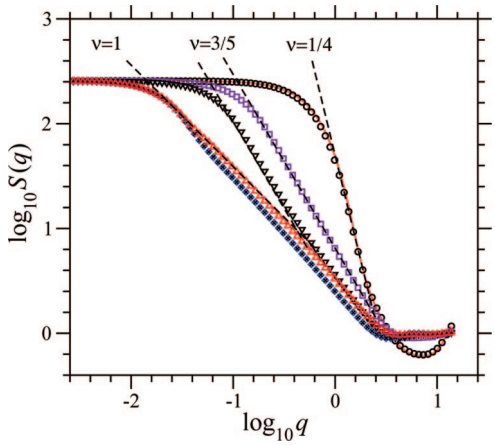

Figure 8. Spherically averaged structure factor ($\tau = 0.07$, $\mu = 8.0$) at varying screening length: $\lambda_D/b_0 = 0.01$ (−), 0.1 (○), 0.3 (□), 1.0 (▽), 10 (◇), 50 (×, inside ◇), 1024 (△). Dashed lines show particular scaling behavior.

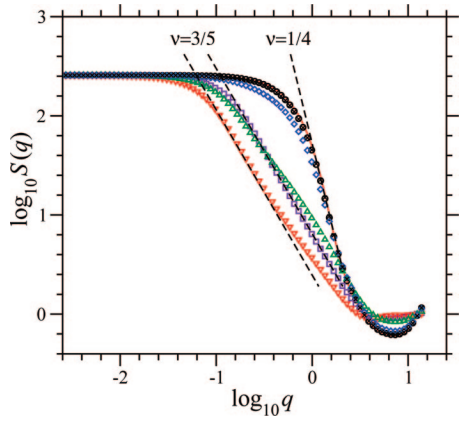

Figure 9. Spherically averaged structure factor ($\tau = 0.07$, $\mu = 2.0$) at varying screening length: $\lambda_D/b_0 = 0.01$ (−), 0.1 (○), 0.3 (□), 1.0 (▽), 4.0 (△), 10 (◇), 256 (×, inside ○). Dashed lines show particular scaling behavior.

Table 2. Recombination Point $\tilde{\lambda}_D$ in the Close-to-Θ-Point Regime ($N = 256$, $\tau = 0.07$)

μ	λ_D^*/b_0
2.0	0.90 ± 0.05
3.0	1.8 ± 0.1
4.0	3.0 ± 0.5
8.0	40.0 ± 4.0

an external control parameter in simulations with varying salt concentration, one models a situation that is different from the experimental setup with pH being the control parameter. To check the influence of the varying self-energy term, we performed additional simulations at constant pH. In Figure 5, the average degree of ionization and chain size are plotted as a function of screening length at $\mu = \text{const} = 5$, $\text{pH} - \text{p}K_0 = \text{const} = 2.17$ and $\mu = \text{const} = 7$, $\text{pH} - \text{p}K_0 = \text{const} = 3.04$. The pH values are chosen to give the corresponding μ at vanishing screening. Therefore, related curves merge at large λ_D. If the chemical potential of the charges is rather large and the coil-to-globule transition appears at large screening lengths, roughly at $\lambda_D/b_0 > 10$, then the correction to μ due to the self-energy term can be neglected. (See eq 6.) Hence, there is almost no shift in the transition. (See $\mu = 7$.) However, for reduced chemical potential or pH, respectively, and with a phase transition occurring at screening lengths on the order of bond length, b, the finite screening causes a finite shift in the transition. In summary, when pH is used as external control

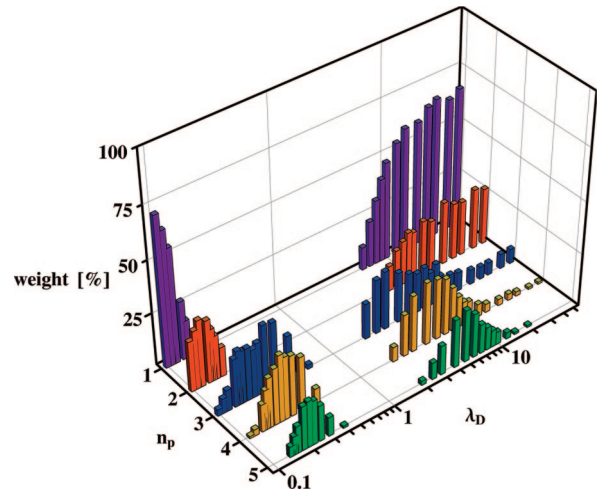

Figure 10. Pearl population ($\tau = 0.07$, $\mu = 2.0$) at varying screening length, λ_D (in units of b_0). n_p is the order (number of pearls) of the configuration.

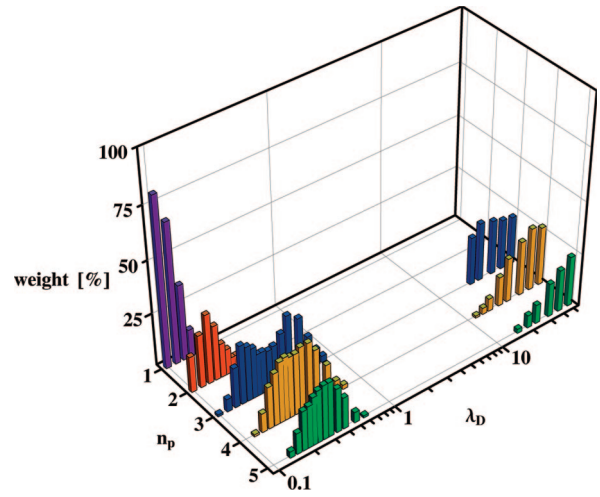

Figure 11. Pearl population ($\tau = 0.07$, $\mu = 4.0$) at varying screening length, λ_D (in units of b_0).

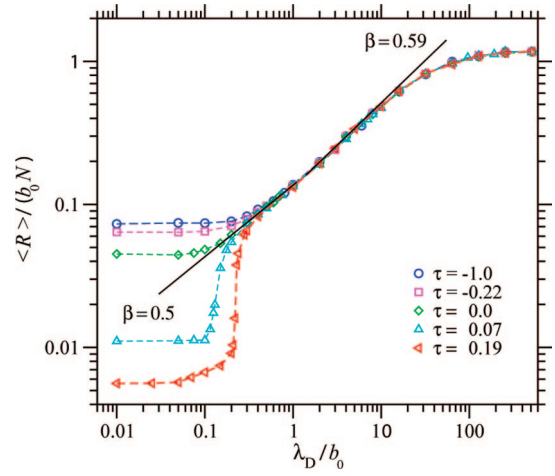

Figure 12. Mean square end-to-end distance as a function of screening length for chains of length $N = 512$ with fixed degree of charging, $f = 1$, at varying solvent quality: $\tau = -1.0$ (○), −0.22 (□), 0 (◇), 0.07 (△), and 0.19 (triangle left).

parameter instead of μ, the dependencies on ionic strength are not qualitatively changed; however, for a specific pH range,

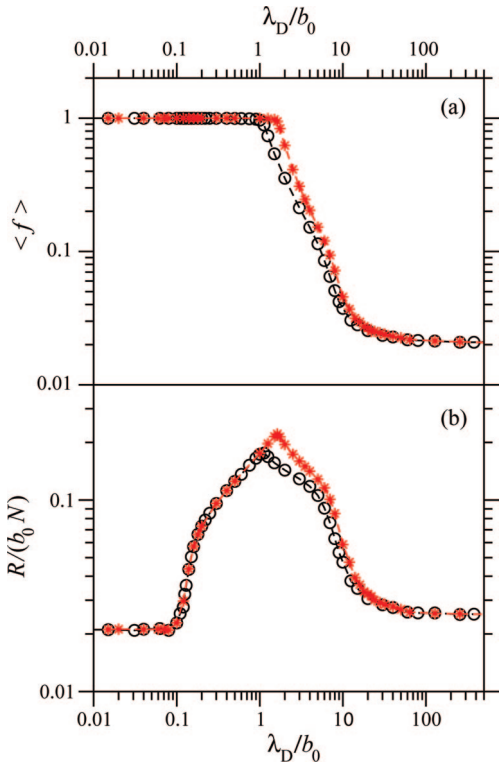

Figure 13. Simulation results at $\tau = 0.07$ ($N = 256$, $\lambda_B = b_0$). Shown are (a) average degree of charging versus screening length and (b) m.s. end-to-end distance versus screening length, both at $\mu = 2$ (○) and $pH - pK_0 = 0.87$ (∗).

there occurs a shift in the critical screening length at which polyelectrolytes undergo the coil-to-globule transition.

4.2. Close-to-Θ-Point Regime. In Figure 6, we plot the degree of charging and mean-square end-to-end distance as a function of screening length, λ_D, at varying chemical potential, μ. Typical simulation snapshots that illustrate chain structure in the different regions are shown in Figure 7. The striking difference from the behavior in the rather-poor-solvent regime discussed above is the absence of discrete transitions. For $\lambda_D > \tilde{\lambda}_D(\mu)$, ionized sites start to recombine, and the average degree of charging, $<f>$, monotonously decreases with growing λ_D. The recombination points, $\tilde{\lambda}_D(\mu)$, are given in Table 2. The larger μ is, the larger is $\tilde{\lambda}_D$; the slower is the decay from the fully ionized state, and the larger is the saturation value of ionization at $\lambda_D \to \infty$. For varying λ_D, the spherically averaged structure factor is plotted in Figures 8 ($\mu = 8$) and 9 ($\mu = 2$). Combining the various data, the following structure model is suggested in the close-to-Θ-point regime. At small and intermediate screening lengths, we obtain three regimes that are very similar to those found in the rather-poor-solvent case: (i) Below $\lambda_D/b_0 = 0.1$, there occurs an unperturbed globule. Because of the better solvent quality, its average size is slightly enlarged and its shape is rather floppy. This is why the structure factor does not exhibit any fingerprint of globule size. (ii) Between $\lambda_D/b_0 = 0.1$ and 0.3, the polyelectrolyte changes its structure from globule to swollen coil with $R \sim N^{3/5}$ at $\lambda_D/b_0 = 0.3$. (iii) For large μ, the scaling behavior of completely charged chains is obtained at $0.3 < \lambda_D/b_0 < 10$. With growing screening length, because of growing persistence length, the chain becomes increasingly stiff on short scales, whereas it preserves the swollen coil structure on large lengths. The width of this particular regime is reduced with growing λ_D. For chain length $N = 256$, it disappears at $\lambda_D/b_0 \approx 10$, where the chain becomes almost homogeneously stretched with $\nu \approx 0.9$. With respect to λ_D, we find a scaling law, $R \sim \lambda_D^{0.52}$, that gives $l_e \sim b(\lambda_D/b)^{1.6}$, that is, within the limits

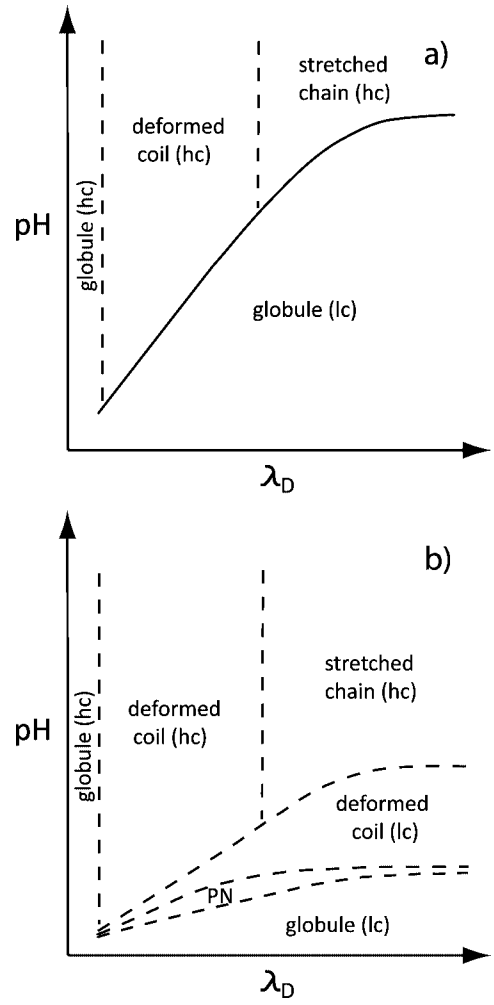

Figure 14. Schematic phase diagram of weak PELs in poor solvent in (a) the rather-poor regime $\tau > \tau_a^*$ and (b) the close-to-Θ-point regime $\tau < \tau_a^*$. The solid line in a) indicates a first-order phase transition between high-charge states (hc) and a low-charge state (lc). Whereas at $\tau > \tau_a^*$, this appears to be a pronounced transition between almost completely charged chains and almost uncharged globules, in the close-to-Θ-point regime, the hc−lc transition is a continuous one. All continuous transitions are represented by dashed lines. Note that hc globules occurring at very strong screening can split into pearl necklaces that are quite different from usual DRO pearl necklaces denoted by PN.

of accuracy equal to the exponent 1.7 obtained above in the rather poor case. Although the chain still remains completely charged, at $\lambda_D/b_0 \approx 10$, the stretching with growing λ_D shows some saturation. This is obviously due to the strong elongation of the chain that is about $^2/_3$ of its contour length. For any nonglobular conformation, at large screening lengths, the chains are not homogeneously stretched. On one hand, they are highly stretched on large length scales reaching $\nu \approx 1$ at $\mu = 8$ (Figure 8), but on the other hand, they become rather wiggled on short scales because of reduced charging. Therefore, the appropriate structure model is given by an elongated chain of electrostatic blobs.

In a previous study,[21] we showed that pearl necklace structures can be tuned by changing the degree of charging of annealed PEL chains caused by a variation of the solution pH (chemical potential of the charges). Here we demonstrate that a fine tuning of the chain structure is attainable by varying f via a changed screening length, λ_D. With our choice of parameters, pearl necklaces exist at a degree of charging on the order of $f \approx 0.1$.[21] Therefore, μ has to be small enough that such an f is reached at least at vanishing screening. Otherwise,

the chain remains in a rather extended and more or less uniformly stretched conformation up to large screening lengths. In Figures 10 and 11, the pearl necklace populations at varying λ_D are shown for $\mu = 2$ and 4, respectively. They are obtained by means of a cluster recognition algorithm.[21,44] For $\mu = 2$, the main pearl necklace regime occurs at about $2 < \lambda_D/b_0 < 20$. With growing λ_D, the degree of charging is reduced, and the pearl distribution is shifted toward a smaller number of pearls. Finally, at $\lambda_D/b_0 > 8$, the leading contribution comes from a single globule. For $\mu = 4$, because of the enhanced charging, only higher order pearl necklace states exist at rather large λ_D. We remember that the pearl necklaces structures in the weakly charged regime discussed so far follow the DRO theory.[29] Surprisingly, pearl necklaces exist in a second region distinguished by complete ionization, $f = 1$, but at very strong screening, $\lambda_D < b_0$, within the accuracy of the cluster recognition algorithm independent of μ. This regime is beyond the scope of the DRO theory. Here the suppression of Coulomb repulsion on small length scales necessary for an inhomogeneous stretching of polyelectrolyte chains is not attained by reduced charging but by increased screening. Note, however, that this is a rather narrow region that is artificially stretched by the logarithmic plot in Figures 10 and 11.

To analyze the influence of solvent quality on the λ_D dependence in the scaling region $0.3 < \lambda_D/b_0 < 10$, we simulate chains with $N = 512$, that is, twice as long as before, at different τ both below and above the Θ point. Because in the λ_D region of interest, the chains are completely charged, in the particular simulations, we assume that the degree of charging is fixed with $f = 1$. In Figure 12, the mean-square end-to-end distance is plotted as a function of screening length, λ_D, for different solvent quality, τ. Note that the Θ point, $\beta_\Theta = 2.596$, which was determined along the route described elsewhere,[20] is slightly shifted compared with $\beta_\Theta = 2.615$ found earlier for chains with $N = 256$. At $\tau = (\beta - \beta_\Theta)/\beta_\Theta = -1$, that is, at $\beta = 0$, the modified Lennard-Jones potential defined in eq 20 becomes purely repulsive and gives the best solvent quality attainable with our choice of ε. Clearly, there are two different regimes. At large screening lengths, roughly at $\lambda_D > b_0$, the chain size is governed by electrostatic excluded volume and obeys a universal scaling, $R \sim \lambda_D^{0.59}$, independent of solvent quality. According to eq 15, the behavior is in good agreement with the Khokhlov−Khachaturian prediction of OSF-like behavior. Below $\lambda_D \approx b_0$, the chain size becomes strongly dependent on solvent quality. In a rather narrow λ_D range, $0.3 < \lambda_D/b_0 < 1$, there is some indication of a different power law behavior. For the θ point, we find an $R \sim \lambda_D^{0.50}$ scaling. Therefore, the different slopes obtained above as an average scaling behavior in the total range $0.3 < \lambda_D/b_0 < 10$ are in fact an artifact due to finite size effects.

In Figure 13, the average degree of ionization and chain size are plotted as a function of screening length at both $\mu = \text{const} = 2$ and at $\text{pH} - \text{p}K_0 = \text{const} = 0.87$. The pH is chosen to give $\mu = 2$ at vanishing screening; that is, the two curves merge at large λ_D. At strong screening, there is no difference because the chains are completely ionized anyway. However, at intermediate screening due to eq 6, charges have a chemical potential that is slightly larger than $\mu = 2$, and the point at which recombination starts is somewhat shifted to larger screening lengths. Considering the whole λ_D range, this effect is weak, and it is reduced with growing pH.

5. Conclusions

By performing extensive grand canonical Monte Carlo simulations of annealed PELs in poor solvents, we have shown that variable screening can be used to establish a fine tuning of the structure of weak PELs. In Figure 14, the results are combined in schematic phase diagrams in both the rather-poor-solvent regime and the close-to-Θ-point regime.

In the rather-poor-solvent regime that is reached at $\tau > \tau_a^*$, even at a solution pH, which is large enough to ensure complete charging at strong screening, $\lambda_D < b$, the stretched chain can be enforced to collapse into an almost uncharged globule by reducing the screening and enlarging the electrostatic penalty the system has to pay for an ionized state. Similarly, the solution pH at which an annealed PEL undergoes the discontinuous transition into a globule can be adjusted by varying the salt concentration, that is, by setting the appropriate screening of the electrostatic interaction. Therefore, the variation of ion strength represents an appropriate tool for shifting the discrete structure transition of annealed PELs into the desired pH range.

In the close-to-Θ-point regime, $\tau < \tau_a^*$, a fine tuning of chain structure can be realized by varying screening. In particular, the population of different pearl necklace configurations can be changed by a variation of screening length, λ_D. However, weakly charged pearl necklace structures described by the DRO theory appear at only low pH if the low ionization regime is reached, with our parameter set corresponding to $f \approx 0.1$. In other words, pearl necklaces do not exist if strong ionization is pinned by a sufficiently high chemical potential of the charges. In addition to pearl necklaces in the usual weakly charged regime, we find similar structures at complete charging but in a narrow window of rather strong screening, $\lambda_D < b$. Here the total electrostatic interaction within a pearl is not suppressed because of partial charging but by strong screening. Obviously, this mechanism is beyond the scope of the DRO theory.

By increasing the Debye length in both poor solvent regimes, we observe an unusual nonmonotonic stretching of PEL chains. This particular feature of annealed PELs appears because the degree of charging is not fixed but becomes increasingly reduced with growing screening length. Therefore, there is a counterpart to the usual polyelectrolyte effect, which is given by an increasing local stiffness described by the electrostatic persistence length and a growing global swelling described by the electrostatic excluded volume that gives rise to the nonmonotonic stretching obtained in the simulations.

At intermediate screening lengths where the interaction is dominated by electrostatic contributions but ionization is yet not affected and still fixed at $f = 1$, after a careful check of finite size effects, we demonstrate the scaling behavior of chain size with respect to screening length to be independent of solvent quality. Using the model of a flexible chain built by cylindrical monomers of length, l_e, and diameter, λ_D, we find good agreement with the Khokhlov−Khachaturian prediction of OSF-like behavior, $l_e \sim \lambda_D^2$.

Acknowledgment. We gratefully acknowledge stimulating discussions with Roland Netz.

References and Notes

(1) Dautzenberg, H.; Jaeger, W.; Kötz, J.; Philipp, B.; Seidel, C.; Stscherbina, D. *Polyelectrolytes: Formation, Characterization and Application*; Hanser Publishers: NewYork, 1994.
(2) Barrat, J.-L.; Joanny, J.-F. *Adv. Chem. Phys.* **1996**, *94*, 1–66.
(3) *Polyelectrolytes with Defined Molecular Architecture*; Schmidt, M., Ed.; Advances in Polymer Science, Vols. *165− 166*; Springer: Heidelberg, Germany, 2003.
(4) Nagasawa, M.; Murase, T.; Kondo, K. *J. Phys. Chem.* **1965**, *69*, 4005.
(5) Anufrieva, E. V.; Birstein, T. M.; Nekrasova, T. N.; Ptitsyn, O. B.; Sheveleva, T. V. *J. Polym. Sci. C* **1968**, *16*, 3519–3531.
(6) Dubin, P.; Strauss, U. P. *J. Phys. Chem.* **1973**, *77*, 1427–1431.
(7) Kötz, J.; Philipp, B.; Pfannemüller, B. *Makromol. Chem.* **1990**, *191*, 1219.
(8) Tirtaatmadja, V.; Tam, K. C.; Jenkins, R. D. *Macromolecules* **1997**, *30*, 3271–3282.
(9) Delben, F.; Paoletti, S.; Porasso, R. D.; Benegas, J. C. *Makromol. Chem. Phys.* **2006**, *207*, 2299–2310.

(10) Wang, S.; Zhao, J. *J. Chem. Phys.* **2007**, *126*, 091104.
(11) Raphael, E.; Joanny, J.-F. *Europhys. Lett.* **1990**, *13*, 623–628.
(12) Castelnovo, M.; Sens, P.; Joanny, J.-F. *Eur. Phys. J. E* **2000**, *1*, 115–125.
(13) Borukhov, I.; Andelman, D.; Borrega, R.; Cloitre, M.; Leibler, L.; Orland, H. *J. Phys. Chem. B* **2000**, *104*, 11027–11034.
(14) Netz, R. R. *J. Phys.: Condens. Matter* **2003**, *15*, 239–244.
(15) Garces, J. L.; Koper, G. J. M.; Borkovec, M. *J. Phys. Chem. B* **2006**, *110*, 10937–10950.
(16) Reed, C. E.; Reed, W. F. *J. Chem. Phys.* **1992**, *96*, 1609–1620.
(17) Sassi, A. P.; Beltrán, S.; Hooper, H. H.; Blanch, H. W.; Prausnitz, J. M.; Siegel, R. A. *J. Chem. Phys.* **1992**, *97*, 8767–8774.
(18) Ullner, M.; Jönsson, B. *Macromolecules* **1996**, *29*, 6645–6655.
(19) Zito, T.; Seidel, C. *Eur. Phys. J. E* **2002**, *8*, 339–346.
(20) Uyaver, S.; Seidel, C. *Europhys. Lett.* **2003**, *64*, 536–542.
(21) Uyaver, S.; Seidel, C. *J. Phys. Chem. B* **2004**, *108*, 18804–18814.
(22) Ulrich, S.; Laguecir, A.; Stoll, S. *J. Chem. Phys.* **2005**, *122*, 094911.
(23) Yamaguchi, T.; Kiuchi, T.; Matsuoka, T.; Koda, S. *Bull. Chem. Soc. Jpn.* **2005**, *78*, 2098–2104.
(24) de Gennes, P.-G. *Scaling Concepts in Polymer Physics*; Cornell University Press: Ithaca, NY, 1985.
(25) Grosberg, A. Y.; Khokhlov, A. R. *Statistical Physics of Macromolecules*; AIP Press: New York, 1994.
(26) Khokhlov, A. R. *J. Phys. A* **1980**, *13*, 979–987.
(27) Rayleigh, L. *Philos. Mag.* **1882**, *14*, 184–186.
(28) Kantor, Y.; Kardar, M.; Li, H. *Phys. Rev. E* **1994**, *49*, 1383–1392.
(29) Dobrynin, A. V.; Rubinstein, M.; Obukhov, S. P. *Macromolecules* **1996**, *29*, 2974–2979.
(30) Minko, S.; Kiriy, A.; Gorodyska, G.; Stamm, M. *J. Am. Chem. Soc.* **2002**, *124*, 3218–3219.
(31) Kirwan, L. J.; Papastavrou, G.; Borkovec, M. *Nano Letters* **2004**, *4*, 149–152.
(32) Khokhlov, A. R.; Khachaturian, K. A. *Polymer* **1982**, *13*, 1742–1750.
(33) Helm, C. A.; Laxhuber, L.; Lösche, M.; Möhwald, H. *Colloid Polym. Sci.* **1986**, *264*, 46–55.
(34) Zhulina, E. B.; Birshtein, T. M.; Borisov, O. V. *Macromolecules* **1995**, *28*, 1491–1499.
(35) de Gennes, P.-G.; Pincus, P.; Velasco, R. M.; Brochard, F. J. *J. Phys. (Paris)* **1976**, *37*, 1461–1473.
(36) Schiessel, H. *Macromolecules* **1999**, *32*, 5673–5680.
(37) Odijk, T.; Houwaart, A. C. *J. Polym. Sci.: Polym. Phys. Ed.* **1978**, *16*, 627–639.
(38) Odijk, T. *J. Polym. Sci.: Polym. Phys. Ed.* **1977**, *15*, 477–483.
(39) Skolnick, J.; Fixmann, M. *Macromolecules* **1977**, *10*, 944–948.
(40) Netz, R. R.; Orland, H. *Eur. Phys. J. B* **1999**, *8*, 81–98.
(41) Everaers, R.; Milchev, A.; Yamakov, V. *Eur. Phys. J. E* **2002**, *8*, 3–14.
(42) Higgs, P. G.; Raphael, E. *J. Phys. I* **1991**, *1*, 1–7.
(43) Lyulin, A. V.; Dünweg, B.; Borisov, O. V.; Darinskii, A. A. *Macromolecules* **1999**, *32*, 3264–3278.
(44) Limbach, H. J.; Holm, C. *J. Phys. Chem. B* **2003**, *107*, 8041–8055.

MA801817J